Global Ecology and Biogeography A Journal of Macroecology

RESEARCH PAPER

Carbon dynamics of terrestrial ecosystems on the Tibetan Plateau during the 20th century: an analysis with a process-based biogeochemical model

Q. Zhuang[1]*, J. He[1,2], Y. Lu[1], L. Ji[3], J. Xiao[1] and T. Luo[2]

[1]*Department of Earth and Atmospheric Sciences and Department of Agronomy, Purdue University, West Lafayette, IN, 47906, USA,* [2]*The Institute of Tibetan Plateau Research, Chinese Academy of Sciences, PO Box 2871, Beijing 100085, China,* [3]*Chengdu Institute of Mountain Hazards and Environment, Chinese Academy of Sciences, Chengdu 610041, China*

*Correspondence: Qianlai Zhuang, Department of Earth and Atmospheric Sciences and Department of Agronomy, Purdue University, CIVIL 550 Stadium Mall Drive, West Lafayette, IN 47907-2051, USA.
E-mail: qzhuang@purdue.edu

ABSTRACT

Aim The Tibetan Plateau accounts for about a quarter of the total land area of China and has a variety of ecosystems ranging from alpine tundra to evergreen tropics. Its soils are dominated by permafrost and are rich in organic carbon. Its climate is unique due to the influence of the Asian monsoon and its complex topography. To date, the carbon dynamics of the Tibetan Plateau have not been well quantified under changes of climate and permafrost conditions. Here we use a process-based biogeochemistry model, the Terrestrial Ecosystem Model (TEM), which was incorporated with a soil thermal model, to examine the permafrost dynamics and their effects on carbon dynamics on the plateau during the past century.

Location The Tibetan Plateau.

Methods We parameterize and verify the TEM using the existing data for soil temperature, permafrost distribution and carbon and nitrogen from the region. We then extrapolate the model and parameters to the whole plateau.

Results During the 20th century, the Tibetan Plateau changed from a small carbon source or neutral in the early part of the century to a sink later, with a large inter-annual and spatial variability due to changes of climate and permafrost conditions. Net primary production and soil respiration increased by 0.52 and 0.22 Tg C year^{-1}, respectively, resulting in a regional carbon sink increase of 0.3 Tg C year^{-1}. By the end of the century, the regional carbon sink reached 36 Tg C year^{-1} and carbon storage in vegetation and soils is 32 and 16 Pg C, respectively. On the plateau, from west to east, the net primary production, soil respiration and net ecosystem production increased, due primarily to the increase of air temperature and precipitation and lowering elevation. In contrast, the decrease of carbon fluxes from south to north was primarily controlled by precipitation gradient. Dynamics of air temperature and associated soil temperature and active layer depth resulted in a higher plant carbon uptake than soil carbon release, strengthening the regional carbon sink during the century.

Main conclusions We found that increasing soil temperature and deepening active layer depth enhanced soil respiration, increasing the net nitrogen mineralization rate. Together with the effects of warming air temperature and rising CO_2 concentrations on photosynthesis, the stronger plant nitrogen uptake due to the enhanced available nitrogen stimulates plant carbon uptake, thereby strengthening the regional carbon sink as the rate of increase net primary production was faster than that of soil respiration. Further, the warming and associated soil thermal dynamics shifted the regional carbon sink from the middle of July in the early 20th century to early July by the end of the century. Our study suggests that soil thermal dynamics should be considered for future quantification of carbon dynamics in this climate-sensitive region.

Keywords

Carbon dynamics, carbon sink, net ecosystem production, net primary production, permafrost, soil thermal model, Terrestrial Ecosystem Model, Tibetan Plateau.

DOI: 10.1111/j.1466-8238.2010.00559.x
www.blackwellpublishing.com/geb

INTRODUCTION

The collision between the Indian plate and the Eurasian continent plate shaped the Tibetan Plateau and its geological features. The Tibetan Plateau is the highest and youngest plateau in the world covering an area of 2.57 million km^2 with an average altitude above 4000 m in low–middle latitudes and accounting for 26.8% of China's land area (Zhang *et al.*, 2002). According to the Chinese climate classification system, the plateau is classified as a 'plateau climate' (Li, 1993), a subtropical to temperate mountain climate. The South Asian monsoon characterizes the wide ranges of temperature and moisture gradients on the Tibetan Plateau. From south-east to north-west, supplies of heat and water decrease gradually, and forest, meadow, steppe and desert ecosystems are consequently developed with time (Zheng, 1996).

The Tibetan Plateau is a unique region on Earth for studying the responses of natural ecosystems to climatic changes because: (1) its vegetation remains relatively undisturbed by human activities, (2) it has a unique local climate due to the monsoon and variable altitude (Feng *et al.*, 1998; Du, 2001), and (3) its ecosystems are sensitive to global climatic change (Luo *et al.*, 2002). In the most recent 600 years, each warm and cold stage in China appeared first on the Tibetan Plateau (Feng *et al.*, 1998). During the period 1980–94, the warmest year also appeared first in the south-eastern Tibetan Plateau (Feng *et al.*, 1998). In the past 40 years, it has been shown that annual mean air temperature on the Tibetan Plateau has increased at a rate of 0.26 °C $decade^{-1}$ in the most recent 40 years, which is much greater than in any other region in China (Du, 2001). A study has demonstrated that the increase in air temperature caused permafrost-dominated areas in the plateau to shrink by 0.1 million km^2 (Wang *et al.*, 2000). Further, the study indicated that the lower altitudinal limit of permafrost in the region has risen 40–80 m. More importantly, the region contains a large amount of soil carbon and its fate is uncertain under changing climatic conditions. In recent years, how the terrestrial ecosystems in the Tibetan Plateau are responding to these climate changes with respect to carbon dynamics has attracted much attention. To date, progress has been made in investigating terrestrial ecosystem productivity and carbon storage (e.g. Luo *et al.*, 1998, 2004; Lu & Ji, 2002; Piao & Fang, 2002; Wang *et al.*, 2002, 2003; Zhou *et al.*, 2004). However, there has been much less investigation of the net carbon budget on the plateau. A limited number of studies on net carbon exchange between the ecosystems and atmosphere in the region have only been conducted at site level (e.g. Kato *et al.* 2004a,b, 2006). Further the existing analyses have not considered the effects of soil thermal and permafrost dynamics as consequences of climate change over the whole of the plateau.

Here we use the field data of soil temperature and carbon and nitrogen fluxes and pools obtained from the plateau to parameterize a process-based biogeochemistry model, the Terrestrial Ecosystem Model (TEM; Zhuang *et al.*, 2003), which was incorporated with a soil thermal model, for the major ecosystem types in the region. We then apply the model and parameterization to the whole of the plateau to examine how climatic changes have affected carbon dynamics during the 20th century. The study also strives to identify the key controls on carbon dynamics in this climate-sensitive region. This study is a significant step towards assessing the role of the Tibetan Plateau in the global carbon cycle and the climate system.

METHOD

Overview

Considerable field measurements of ecosystem carbon pool sizes and fluxes and soil thermal regimes have been conducted on the Tibetan Plateau, and the characteristics of vegetation and soils of the key ecosystem types have also been well documented (e.g. Paetzold *et al.*, 2003; Luo *et al.*, 2004, 2005a,b). In this study, we used these data and the TEM biogeochemistry model to quantify the changes in carbon fluxes and pool sizes in the region. Below, we first describe the TEM model and its applicability to the region. We then discuss how the model was parameterized using the field data collected on the plateau. Third, we describe how the model and parameters were verified with the measurements for major ecosystem types in the region. Finally, we describe how we applied the model and parameterizations to the plateau to analyse its carbon dynamics in response to changes in climate and atmospheric CO_2 during the 20th century.

The Terrestrial Ecosystem Model (TEM)

The TEM is a process-based, global-scale ecosystem model that uses spatially referenced information on climate, elevation, soils and vegetation to make monthly estimates of carbon and nitrogen fluxes and pool sizes of the terrestrial biosphere (Zhuang *et al.*, 2003). In this study, we used the version of TEM that was coupled with dynamics of freeze and thaw for permafrost- and non-permafrost-dominated ecosystems (Zhuang *et al.*, 2001, 2002, 2003). This version of TEM has been extensively used to evaluate carbon dynamics in northern high latitudes (e.g. Euskirchen *et al.*, 2006; Zhuang *et al.*, 2006; Balshi *et al.*, 2007).

In TEM, for each monthly time step, net ecosystem production (NEP) is calculated as the difference between net primary production (NPP) and heterotrophic respiration (R_H). NPP is calculated as the difference between gross primary production (GPP) and plant autotrophic respiration (R_A). The algorithm for calculating R_A has been described elsewhere (Raich *et al.*, 1991; McGuire *et al.*, 1992, 1997). Monthly GPP considers the effects of several factors and is calculated as:

$$\begin{aligned}\mathrm{GPP} = {} & C_{\max} f(\mathrm{PAR}) f(\mathrm{phenology}) f(\mathrm{foliage}) \\ & f(T) f(C_a, G_v) f(\mathrm{NA}) f(\mathrm{FT})\end{aligned}$$

where C_{max} is the maximum rate of carbon assimilation, PAR is photosynthetically active radiation and *f*(phenology) is monthly leaf area relative to leaf area during the month of maximum leaf area and depends on monthly estimated evapotranspiration

Table 1 Soil thermal model parameters for tundra and forest ecosystems on the Tibetan Plateau.

Parameter	Tundra	Forest	Unit
Upper organic soil thickness	0.22	0.20	m
Lower organic soil thickness	0.50	0.35	m
Upper mineral soil thickness	1.00	1.00	m
Upper organic soil thawed thermal conductivity	2.50	1.25	W m^{-1} K^{-1}
Upper organic soil frozen thermal conductivity	1.50	0.26	W m^{-1} K^{-1}
Lower organic soil thawed thermal conductivity	1.70	1.70	W m^{-1} K^{-1}
Lower organic soil frozen thermal conductivity	2.00	0.80	W m^{-1} K^{-1}
Upper mineral soil thawed thermal conductivity	1.50	1.20	W m^{-1} K^{-1}
Upper mineral soil frozen thermal conductivity	2.50	2.10	W m^{-1} K^{-1}
Upper organic soil water content	0.34	0.34	Volumetric %
Lower organic soil water content	0.45	0.45	Volumetric %
Upper mineral soil water content	0.43	0.43	Volumetric %
Upper organic soil thawed heat capacity	1.50	1.70	MJ m^{-3} K^{-1}
Upper organic soil frozen heat capacity	1.20	1.50	MJ m^{-3} K^{-1}
Lower organic soil thawed heat capacity	2.60	2.60	MJ m^{-3} K^{-1}
Lower organic soil frozen heat capacity	2.40	2.40	MJ m^{-3} K^{-1}
Upper mineral soil thawed heat capacity	3.10	3.10	MJ m^{-3} K^{-1}
Upper mineral soil frozen heat capacity	1.70	1.70	MJ m^{-3} K^{-1}

The full definition of parameters is in Zhuang *et al.* (2001).

(Raich *et al.*, 1991). The function *f*(foliage) is a scalar function that ranges from 0.0 to 1.0 and represents the ratio of canopy leaf biomass relative to the maximum leaf biomass (Zhuang *et al.*, 2002), T is monthly air temperature, C_a is atmospheric CO_2 concentration, G_v is relative canopy conductance and NA is nitrogen availability. The effects of elevated atmospheric CO_2 directly affect $f(C_a, G_v)$ by altering the intercellular CO_2 of the canopy (McGuire *et al.*, 1997; Pan *et al.*, 1998). The function *f*(NA) models the limiting effects of plant nitrogen status on GPP (McGuire *et al.*, 1992). The function of *f*(FT) describes the effects of freeze–thaw dynamics on GPP. In TEM, two freezing fronts are modelled, including freezing down due to cold air temperature and freezing-up due to permafrost underneath the soils (Zhuang *et al.*, 2001). As a result, the soil temperature profile is more accurately simulated than without considering permafrost conditions. R_H is calculated based on modelled soil temperatures by considering permafrost dynamics. More details of how GPP and R_H are calculated by considering permafrost dynamics can be found in Zhuang *et al.* (2003). In this version of the TEM, we modelled the net nitrogen mineralization rate (NETNMIN) as a function of soil temperature changes in the top 20 cm of soils. Thus, the effects of changing permafrost conditions on soil thermal regimes will influence not only soil decomposition rate but also the nitrogen mineralization rate, and thus the available nitrogen and the rate of nitrogen uptake by vegetation (Zhuang *et al.*, 2003).

Model parameterization

The TEM requires the use of monthly climatic data and soil- and vegetation-specific parameters associated with the soil and vegetation carbon and nitrogen processes. Although many of the parameters in the model are defined from published information (e.g. Raich *et al.*, 1991; McGuire *et al.*, 1992; Zhuang *et al.*, 2003), some are determined by calibrating the model to fluxes and pool sizes of intensively studied field sites. For this application of the TEM, we developed a set of parameters for soil thermal dynamics and carbon and nitrogen processes specifically for the Tibetan Plateau for various ecosystem types based on field data collected in the region. Monthly air temperature and precipitation of the six calibration sites used in this study are multi-year averages based on the local meteorological observations on the Tibetan Plateau (Luo *et al.*, 2004).

To parameterize the soil thermal dynamics of Tibetan Plateau ecosystems, we parameterized tundra and boreal forest ecosystems based on field data of soil temperatures for depths of 10, 20, 50 and 100 cm at the Fenghuoshan and Gongga sites, respectively. The parameterization was conducted by minimizing the differences between observed and simulated soil temperature at these depths. The parameters of soil thermal conductivity and heat capacity are documented in Table 1. The carbon and nitrogen dynamics of the TEM were then parameterized for major ecosystem types including wet tundra, boreal forest, mixed temperate forest, temperate deciduous forest, boreal woodlands and alpine tundra. For each ecosystem type, we used the measured data of pool sizes of vegetation carbon, soil carbon, vegetation nitrogen, soil nitrogen and annual NPP fluxes for calibration (see Appendix S1 in Supporting Information).

Site-level verification

Four alpine tundra and boreal forest ecosystem sites were selected to verify our parameterization for soil thermal dynamics. At these sites, the soil temperature profile was observed at

Table 2 Comparison between the observed and simulated monthly temperature for each soil layer at different sites on the Tibetan Plateau.

Site name	Longitude (degrees)	Latitude (degrees)	Elevation (m)	Vegetation type in TEM	R^2 values for each layer 10 cm	20 cm	50 cm	100 cm	Periods
Wuli	92.7	34.5	4597	Alpine tundra	0.96	0.95	0.87	0.71	Sept. 1999–Dec. 2000
Fenghuoshan	92.9	34.7	4760	Alpine tundra	0.94	0.92	0.78	0.48	June 1998–Dec. 2000
Liangdaohe	91.7	31.8	4850	Alpine tundra	0.96	0.95	0.84	0.58	Oct. 1999–July 2000
Gongga	102.0	29.5	3000	Boreal forest	0.91	0.89	0.84	0.64	Jan. 1998–Dec. 1999

TEM, Terrestrial Ecosystem Model.

Table 3 Characteristics of verification sites for the Terrestrial Ecosystem Model (TEM) parameters used in this study.

Site name*	Longitude (degrees)	Latitude (degrees)	Elevation (m)	Annual precipitation (mm)	Annual temperature (°C)	Soil texture (%) Sand	Silt	Clay	Vegetation type in TEM
Wudaoliang (WDL)	93.07	35.22	4626	270.3	−4.2	91	6	3	Alpine tundra
Tuotuohe (TTH)	92.55	34.31	4582	301.3	−3.9	97	2	1	Alpine tundra
Damxung (DX)	91.15	30.50	4288	486.9	−0.1	53	32	15	Alpine tundra
Gandansi (GDS)	91.49	29.75	4100	488.0	3.1	49	36	15	Alpine tundra
Nagqu (NQ)	91.93	31.57	4636	468.7	−2.6	62	28	10	Alpine tundra
Haibei (HB)	101.31	37.56	3280	547.7	−1.0	70	17	13	Alpine tundra
Perk of Sergyla Mt (PSM)	94.65	29.61	4560	722.7	0.4	49	42	9	Wet tundra
Maizhogongka (MZG)	91.63	29.80	3780	445.8	5.0	68	22	10	Wet tundra
Gongga Mt site 4 (GG4)	102.00	29.58	3000	1926.0	4.0	82	11	7	Boreal forest
Gongga Mt site 6 (GG6)	101.97	29.55	3700	2384.7	−0.2	74	16	10	Boreal forest

TEM, Terrestrial Ecosystem Model.
*Items in parentheses are abbreviation of the site names. The information for these sites is based on our field studies (Luo *et al.*, 2002, 2004, 2005a,b).

depths of 10, 20, 50 and 100 cm (Table 2). We also used the observed data for carbon and nitrogen pools and fluxes at different sites from those used for calibration to verify the TEM parameterization. The verification sites included six alpine tundra ecosystems, two wet tundra ecosystems and two boreal forest ecosystems (Table 3). These sites represent the key ecosystem types in the region, and details of their climate, elevation, soils and geographical locations are organized based on our field data and previous studies (Luo *et al.*, 2002, 2004, 2005a,b). We applied the parameterization of alpine tundra, wet tundra and boreal forests and the TEM to conduct simulations for those 10 ecosystems for the period of 1940–2000. The monthly precipitation, air temperature and cloudiness from 1940 to 2000 extracted from the UK Climate Research Unit (CRU) data sets were used in our simulation (Mitchell & Jones, 2005). The measured NPP, vegetation carbon, soil carbon, vegetation nitrogen and soil nitrogen were compared with TEM estimates. To conduct the comparison, the simulated carbon and nitrogen fluxes and pools were aggregated to decadal averages for the 1990s.

Regional simulations

We conducted two sets of regional simulations; one considered the effects of soil thermal dynamics (hereafter referred to as 'on') and the other did not (hereafter referred to as 'off'). Specifically, in the 'on' simulations, R_H and NETNMIN were calculated based on modelled soil temperatures by considering permafrost dynamics and GPP was modelled a function of freeze–thaw dynamics (Zhuang *et al.*, 2003). In contrast, in the 'off' simulations, these carbon and nitrogen fluxes were modelled as functions of air temperature. To conduct these simulations, we first organized the atmosphere, vegetation, soil texture and elevation data at a resolution of 8 km × 8 km from 1901 to 2002. Specifically, the monthly air temperature, precipitation and cloudiness were based on data from the CRU (Mitchell & Jones, 2005). These data were then resampled to an 8 km × 8 km spatial resolution from the original 0.5° × 0.5° resolution. The annual atmospheric CO_2 data for the period 1901–2002 required for driving the TEM were from our previous studies (Zhuang *et al.*, 2003). The vegetation data over the Tibetan Plateau were derived from the International Geosphere-Biosphere Program (IGBP) Data and Information System (DIS) DISCover Database (Belward *et al.*, 1999; Loveland *et al.*, 2000). The 1 km × 1 km DISCover dataset was reclassified to the TEM vegetation classification scheme (Melillo *et al.*, 1993) and then aggregated to an 8 km × 8 km spatial resolution. The soil texture data were based on the Food and Agriculture Organization/Civil Service Reform Committee (FAO/CSRC) digitization of the FAO-UNESCO (1971) soil map. The soil texture data were resampled from

0.5° × 0.5° to 8 km × 8 km. For elevation, we used the 1 km × 1 km elevation data derived from the Shuttle Radar Topography Mission (SRTM) (Farr *et al*., 2007). The SRTM data were also resampled to match the resolution of climate, vegetation and soil texture data.

For both regional simulations, we first ran the TEM to equilibrium for an undisturbed ecosystem using the long-term averaged monthly climate data from 1901 to 2002 for each grid cell. We then spun up the model for 120 years with the climate from 1901 to 1940 to account for the influence of inter-annual climate variability on the initial conditions of the undisturbed ecosystem. We then ran the model with transient monthly climate and atmospheric CO_2 data from 1901 to 2002.

RESULTS

Site-level studies

The parameterized TEM is able to reproduce the observed soil temperature profile for each verification site (Table 2). The model performs better in soil layers shallower than 50 cm ($R^2 > 0.78$, $P < 0.01$, $n = 31$) and slightly deviates from observation at 100 cm depth ($R^2 > 0.48$, $P < 0.01$, $n = 31$) probably due to our prescribed soil moisture. Prescribed soil moisture in different layers may be different from real conditions in the field, which affects soil thermal conductivity and heat capacity, and thus the soil thermal dynamics.

Our simulated pool sizes of carbon and nitrogen and annual NPP are comparable to the observed data (Fig. 1). Specifically, for vegetation carbon, TEM simulation is correlated well with the observations ($R^2 = 0.91$, $P < 0.01$, $n = 10$). Except at Nagqu and Gongga Mountain sites 4 and 6, model simulations compare well with observations at the rest of sites. Likewise, the simulated vegetation nitrogen is similar to the observations ($R^2 = 0.86$, $P < 0.01$, $n = 10$). The model underestimates at Nagqu, but overestimates at Gongga Mountain sites 4 and 6 as well as Perk of Sergyla Mountain and Maizhogongka. In contrast, the simulated soil carbon and nitrogen pools agree with the observations ($R^2 < 0.32$, $P < 0.01$, $n = 10$). For soil carbon, the model is able to reproduce the observations at Wudaoliang, Tuotuohe, Gandansi and Gongga Mountain site 4. For soil nitrogen, the model underestimates at Nagqu, Haibei and Gongga Mountain site 6, but overestimates at Perk of Sergyla Mountain and Maizhogongka. The discrepancy between carbon and nitrogen simulations and our observations may be due to the underestimates of these pools in our parameterization sites, leading to lower values in these verification sites. This suggests that we should be cautious in interpreting our regional simulations of these pools. For NPP, if we pool together the simulated average annual NPP of all 10 sites for the 1990s, the comparison indicates that the model simulations are comparable to the observed annual NPP ($R^2 = 0.56$, $P < 0.01$, $n = 10$).

Regional soil thermal and moisture dynamics

TEM simulation shows that the total area of permafrost distribution is 1.52 million km^2. We used the simulated soil temperatures at 100 cm depth to determine the permafrost states. Specifically, if the soil temperature of a model grid cell is below 0.0 °C at this depth for two consecutive years during the summer, the grid cell is treated as permafrost underneath.

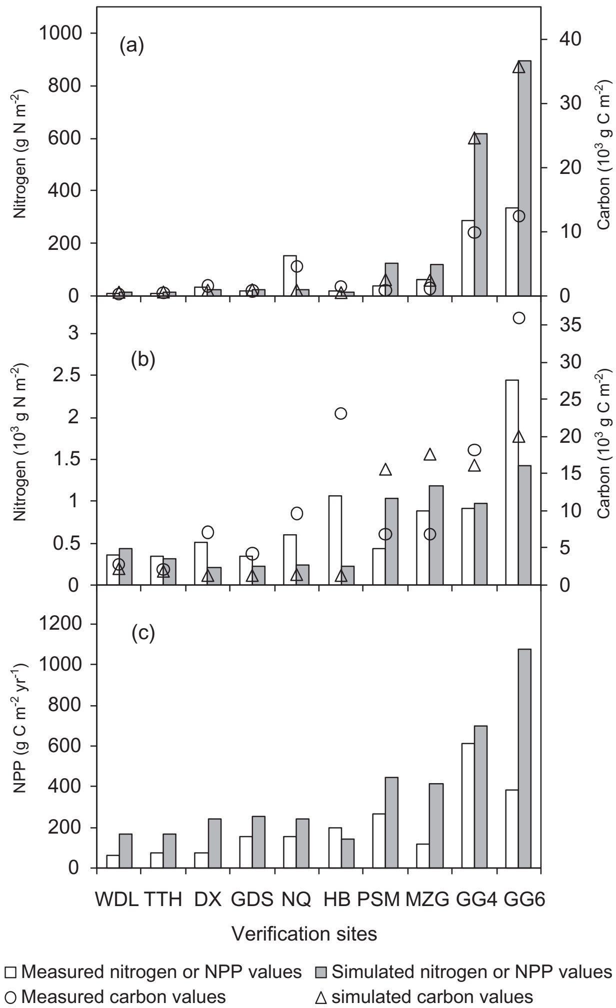

Figure 1 Verification of the Terrestrial Ecosystem Model (TEM) parameterization of various ecosystem types in the Tibetan Plateau for (a) vegetation, (b) soils and (c) net primary production (NPP). The coefficients of determination (R^2) for the comparisons between the observed and simulated data are 0.56 for NPP, 0.23 for soil carbon, 0.42 for soil nitrogen, 0.91 for vegetation carbon and 0.86 for vegetation nitrogen. For site abbreviations see Table 3.

Our simulated permafrost distribution is comparable with the existing data (Fig. 2). Specifically, Brown *et al*. (1998) estimated that the region contains a total of 1.66 million km^2 of permafrost land, including 300 km^2 of continuous permafrost, 0.92 million km^2 of discontinuous permafrost, mostly in the interior of Tibet, 0.05 million km^2 of isolated permafrost and 0.69 million km^2 of sporadic permafrost spreading in areas at the edge of Tibet (Fig. 2a). Qiu *et al*. (2002) estimated a total permafrost area of 1.68 million km^2, which includes 0.86 million km^2 of predominantly continuous permafrost, 0.52 million km^2 of predominantly continuous and island permafrost and

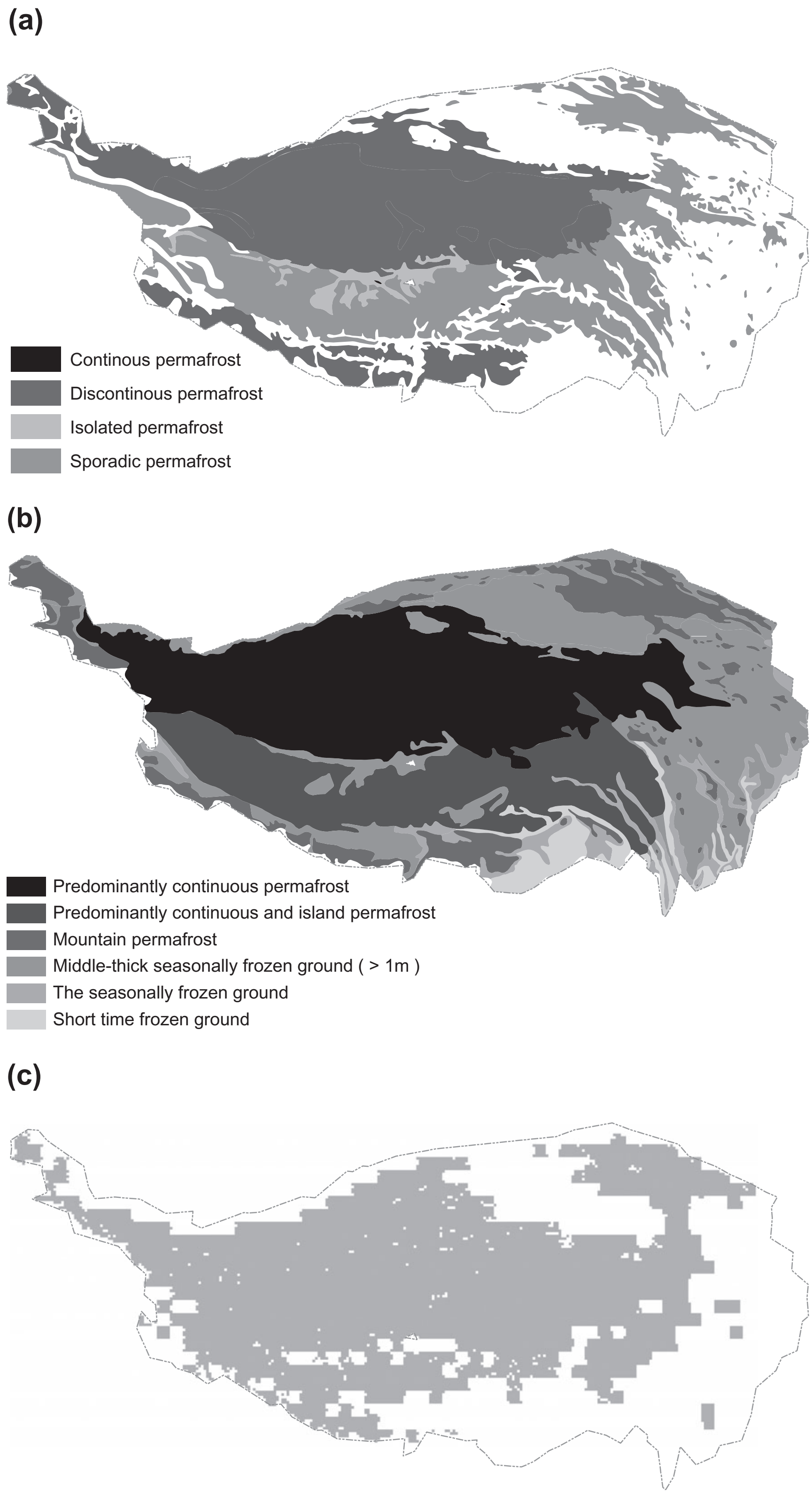

Figure 2 (a) Permafrost distribution from Brown *et al.* (1998) (b) Permafrost distribution from Qiu *et al.* (2002). (c) Current permafrost distribution simulated with the Terrestrial Ecosystem Model (TEM).

0.3 million km^2 of mountain permafrost (Fig. 2b). TEM simulations also agree well with the data with respect to the geographic distribution of permafrost (Fig. 2c).

As to soil thermal regimes including changes of soil temperatures and active layer depths during the 20th century, our simulations are also comparable with other studies. At the 50 cm soil depth, our simulated soil temperature increases 0.5 °C from the 1970s to the 1990s. This is consistent with the finding of Wang *et al.* (2000) that there was a 0.1–0.5 °C increase in the annual ground temperature. Our simulated spatial patterns of active layer depths in recent decades are also comparable with a model study of Oelke & Zhang (2007).

Our simulations indicate that the annual soil temperatures in the top 20 cm are mostly below 0.0 °C, with an increasing trend in response to the increase in air temperature through the 20th century (Fig. 3a,d). The rate of increase of the soil temperature is 0.02 °C year^{-1} from 1970 to 2002 ($R^2 = 0.36$; $P < 0.001$, $n = 33$). At a soil depth of 50 cm, our simulated soil temperature increases by 0.5 °C from the 1970s to the 1990s. The region has significant spatial variability in soil temperature with an increasing trend spanning different decades (data not shown). Specifically, the averaged soil temperature in the top 20 cm increased in the interior of the Tibetan Plateau dominated by discontinuous permafrost. The simulated regional maximum active layer depth fluctuates around 3.25 m, with a slight increase corresponding to an increase in air temperature in recent years (Fig. 3a,e). From 1973 to 2002, the region had more areas with deeper active layer depths compared with the period 1901–30, due to warming (Fig. 4).

As a consequence of warming air temperature, the regional soil moisture shows a drying trend in the region while precipitation shows no significant changes (Fig. 3b,c). Spatially, the drying trend evidently appeared in the interior of the Tibetan Plateau; volumetric soil moisture in many areas decreased from 50–60% in the 1930s to a level of 40–50% in the 1990s (data not shown).

Regional carbon dynamics

TEM simulations indicate that the Tibet Plateau acted as a carbon sink of 35.8 Tg C year^{-1} during the 1990s (Table 4). This sink is the difference between the NPP of 451.6 Tg C year^{-1} and R_H of 415.8 Tg C year^{-1} in the total vegetated area of 1.4 million km^2. Tall grasslands with an area of 1.0 million km^2 dominated the regional sink, and were responsible for 90% of the total sink. Short grasslands and mixed temperate forests contributed the second largest sink of 0.9 Tg C year^{-1} each. Boreal forest, boreal woodland and temperate deciduous forests contributed less than 0.5 Tg C year^{-1} to the total sink. Without considering the effects of permafrost dynamics, TEM underestimates the sink by 5 Tg C year^{-1} primarily due to underestimates of NPP (Table 4). The simulated GPP is 948.8 g C m^{-2} year^{-1} during the 1990s (Table 4). Our simulated R_H ranges from 0.1 to 342 Tg C year^{-1} for different ecosystems (Table 4).

During the 20th century, the Tibetan Plateau exhibited a significant inter-annual variability of carbon dynamics (Fig. 3f–h). Overall, the regional sink slightly increased due to warming climate and rising CO_2 concentrations (Fig. 3a,g). Consequently, the regional vegetation and soil carbon increased (Fig. 3i,j). TEM estimates of the regional vegetation and soil carbon were 32 and 16 Pg C, respectively, during the 1990s (Table 4).

In response to the climatic changes of the 20th century, the regional carbon sink shifted from the middle of July in the 1920s to early July in the 1990s (Fig. 5a). In contrast, without considering the effects of soil thermal dynamics in TEM simulations, the seasonal trend of this shift was less obvious (Fig. 5b). Further, the simulated annual carbon sink has an increase trend from the 1920s to the present when soil thermal effects are considered. However, TEM does not show the same trend if soil thermal effects are switched off in simulations. In addition, two different simulations present different sink strengths in the 1990s.

Our simulations indicate that there was great spatial variability in the strength of the sink or source in the region (Fig. 6). From the 1930s to the 1990s, the regional sink became stronger due to an increasing sink in some areas and a decreasing source in other areas. In general, the northern Tibetan Plateau acted as a carbon source while the ecosystems gradually become a carbon sink towards the south. There was also a general trend of carbon source to sink moving from west to east across the plateau.

DISCUSSION

We made extensive use of the observed carbon and nitrogen data and meteorological and ecological data in this region to examine how carbon dynamics have been affected by changes in climate and permafrost during the 20th century. This study represents the first effort to explicitly consider the effects of permafrost dynamics on carbon cycling in this region that is unique because of its diverse vegetation types, high altitudes and Asian monsoon climate. Below we first discuss our simulated carbon dynamics compared with other estimates. Second, we discuss how the regional carbon dynamics have been affected by changes in soil thermal and moisture regimes on the plateau as a whole. Finally we discuss how a set of gradients of altitudes, air temperature and precipitation influence carbon dynamics on different transects. Through the discussion, we strive to identify the key controls of carbon dynamics in the region.

Comparison between our simulated carbon dynamics and other studies

On the plateau, the net ecosystem carbon exchanges have only been observed at a few sites. For example, Kato *et al.* (2006) estimated that alpine meadow ecosystems sequestered carbon at a rate of 78.5 to 192.5 g C m^{-2} year^{-1} from 2002 to 2004 based on eddy covariance measurements. In comparison, TEM estimates a much lower grassland carbon sink of 28 g C m^{-2} year^{-1} during the 1990s over the whole plateau. In contrast, our estimated regional NPP is higher than other estimates ranging between 173 and 302 Tg C year^{-1} (Piao & Fang, 2002; Wang *et al.*, 2003; Zhou *et al.*, 2004; Piao *et al.*, 2006). On a per unit area basis,

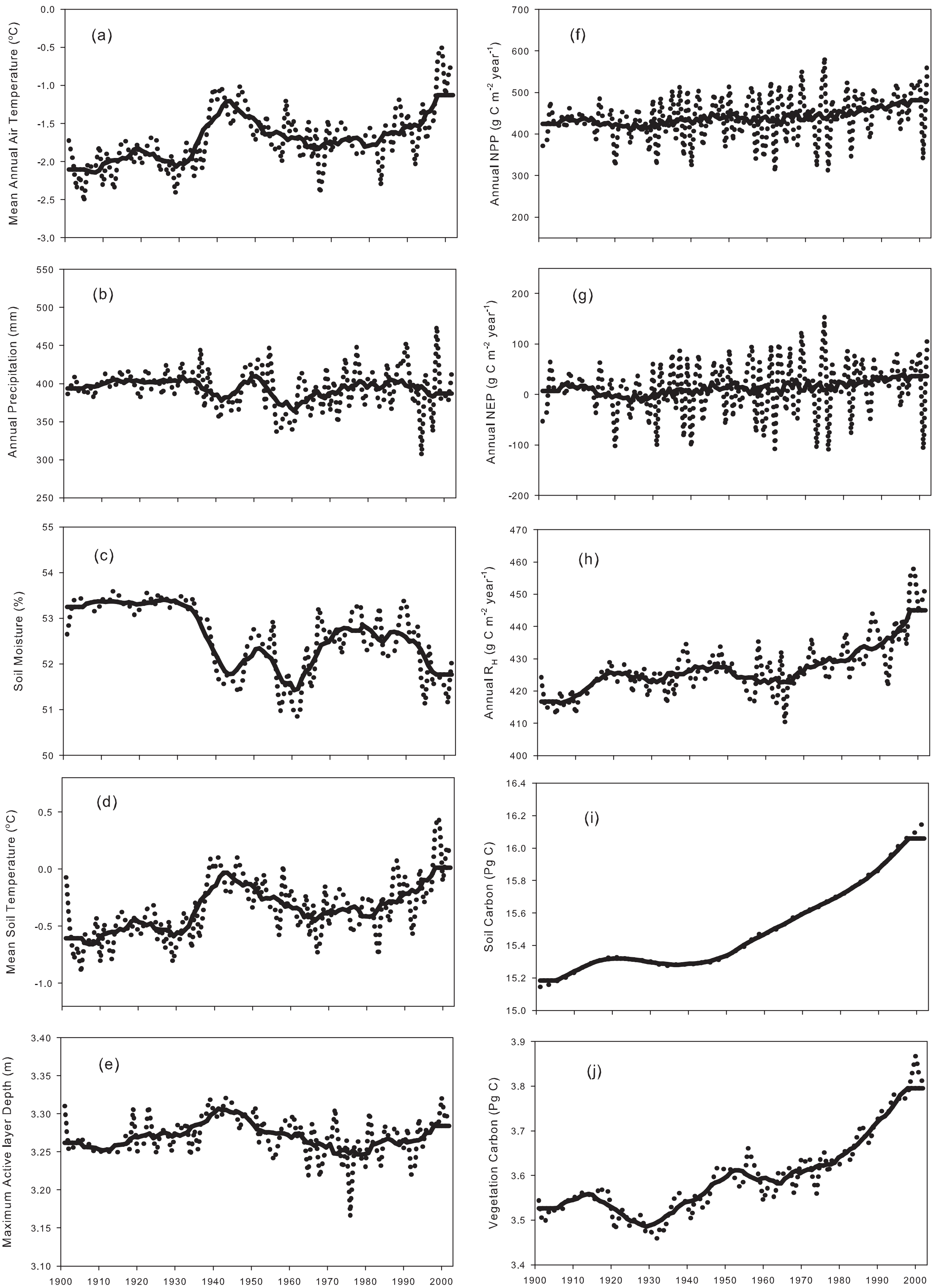

Figure 3 Interannual variability on the Tibetan Plateau for (a) surface air temperature, (b) annual precipitation, (c) soil moisture, (d) soil temperature at top 20 cm depth, (e) maximum active layer depth, (f) net primary production (NPP), (g) net ecosystem production (NEP), (h) heterotrophic respiration (R_H), (i) soil carbon and (j) vegetation carbon. The dark thicker lines are 5-year running averages to show the trends.

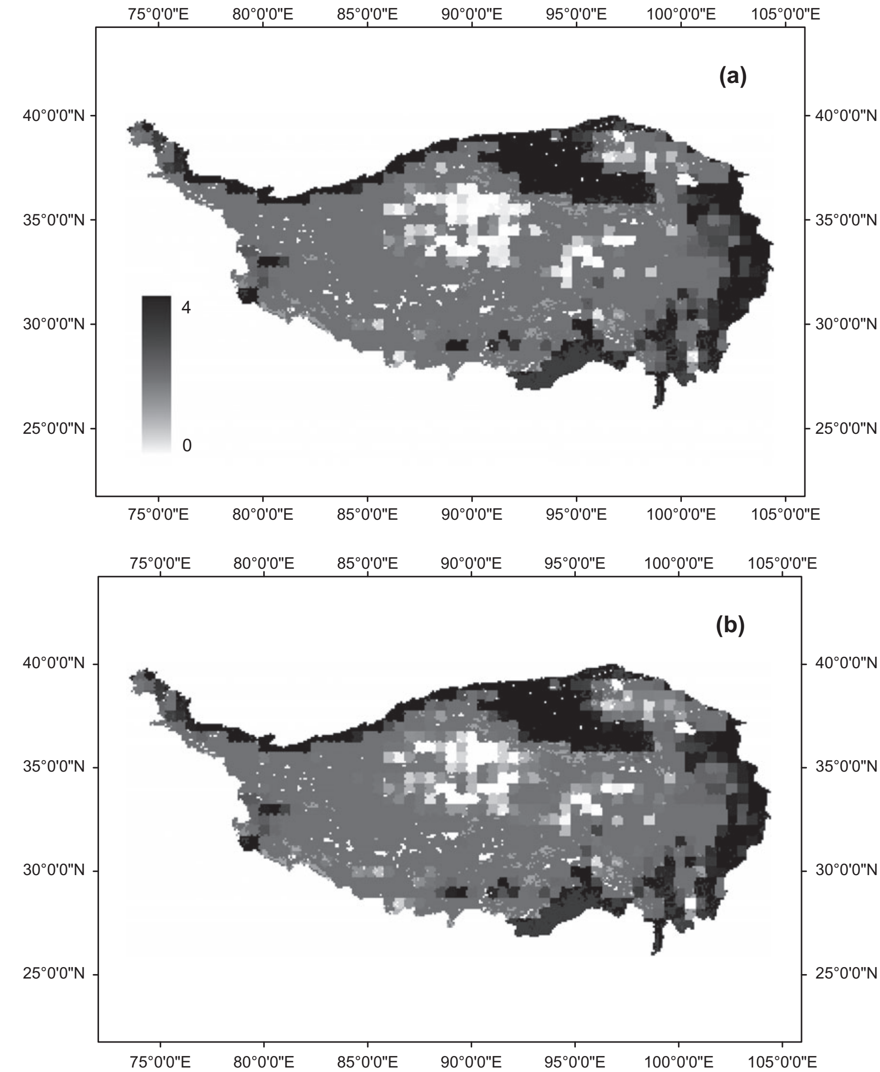

Figure 4 Simulated maximum active layer depth (in m) during the periods (a) 1901–30 and (b) 1973–2002. The values are multiple-year averages.

Table 4 Carbon fluxes (Tg C year^{-1}) and pool sizes (Tg C) of major ecosystem types on the Tibetan Plateau during the 1990s.

	Area	NEP		NPP		R_H		GPP		C_s		C_v	
	(10^3 km^2)	On	Off	On	Off	On	Off	On	Off	On	Off	On	Off
Short grassland	193.9	0.9	0.8	34.6	38.3	33.7	37.5	74.1	80.6	191.4	219.5	131.5	145.6
Tall grassland	1032.6	33.6	29.0	375.6	308.4	342.0	279.4	802.7	659.8	14,679.8	12,158.8	2109.2	1728.9
Boreal forest	0.2	0.0	0.0	0.1	0.1	0.1	0.1	0.2	0.2	2.1	1.8	3.7	3.4
Boreal woodland	78.9	0.2	0.2	7.7	8.6	7.4	8.4	13.4	15.0	229.7	247.4	48.2	51.8
Temperate deciduous forests	46.3	0.2	0.2	8.0	8.2	7.8	8.0	16.0	16.3	200.0	172.1	166.9	170.3
Mixed temperate forests	19.8	0.9	0.8	25.6	23.5	24.7	22.7	42.4	39.8	360.7	290.4	695.6	673.2
Total	1371.6	35.8	31.0	451.6	387.0	415.8	356.0	948.8	811.6	15,663.7	13,090.1	3155.2	2773.2

C_v is total vegetation carbon and C_s is total soil carbon for the region. NEP, NPP, R_H and GPP are net ecosystem production, net primary production, heterotrophic respiration and gross primary production, respectively. 'On' indicates that the Terrestrial Ecosystem Model (TEM) simulation has considered the effects of permafrost dynamics while 'Off' indicates that the effects have not been considered.

TEM-simulated NPP is 330 g C m^{-2} year^{-1} on the Tibetan Plateau, which is close to the regional average of 301 g C m^{-2} year^{-1} estimated by Luo *et al.* (1998) and within the range of estimates of 220–810 g C m^{-2} year^{-1} for various ecosystems in the region by Ni (2000) using the BIOME3 model. Other estimates can reach 500 g C m^{-2} year^{-1} in the south-east and less than 50 g C m^{-2} year^{-1} in the north-west (Lu & Ji, 2002). Our estimated annual NPP persistently increases during the 1980s

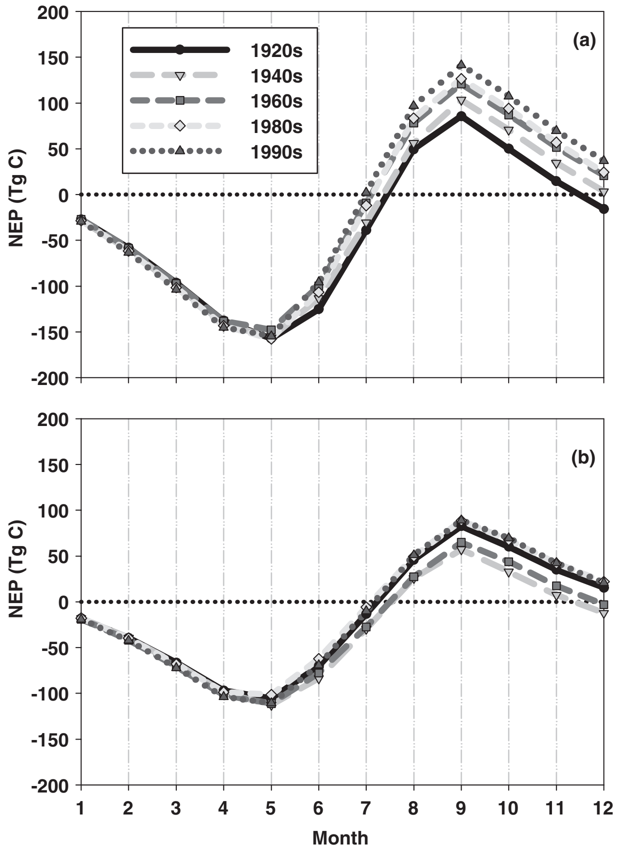

Figure 5 Cumulative monthly net ecosystem production (NEP) on the Tibetan Plateau during the 20th century: (a) considering and (b) without considering the effects of the soil thermal dynamics.

and 1990s (Fig. 3f). Similarly, Piao *et al.* (2006) found a similar trend with a rate of increase of 0.7% year^{-1} from 1982 to 1999. For GPP, Kato *et al.* (2004a) estimated GPP of the alpine meadow ecosystem as 575 g C m^{-2} year^{-1} compared with our estimates of 712 g C m^{-2} year^{-1} for grasslands. In comparison to the estimates based on MODIS data, our simulation tends to underestimate the annual GPP (Li *et al.*, 2007).

TEM estimates of vegetation carbon were much higher than other existing estimates (Table 4). Luo *et al.* (1998) estimated that the Tibetan region has a total of 770 Tg C stored in a vegetated area of 1.1 million km^2. Our much higher estimate of regional vegetation carbon is partially due to parameterization with limited observational data. Verification of the model and parameterization has already shown that the simulated vegetation carbon values in Gongga Mountain sites 4 and 6 are both significantly higher than observations (Fig. 1). The maximum value of 9830 g C m^{-2} appears in Luo *et al.* (1998) at Motuo in the south-east Tibetan Plateau, which is similar to our simulations for the same region (data not shown).

In contrast to vegetation carbon, our simulated soil carbon is much lower than the estimates of 33.5 Pg C at above 1 m soil depth in an area of 1.6 million km^2 (Wang *et al.*, 2002), and 38.4 Pg C at above 0.7 m soil depth in an area of 1.8 million km^2 (Fang *et al.*, 1996). Their studies indicated that most of the soil carbon was stored in alpine meadow and steppe soils. TEM simulations indicate that most soil carbon was stored in tall grasslands (Table 4). The underestimates of soil carbon are due to model parameterization, which was conducted using limited data for soil carbon. Site-level verification of the model and parameters has also indicated that the TEM significantly underestimated soil carbon at Haibei and Gongga Mountain site 6 (Fig. 1).

Due to lower values of soil carbon used in TEM simulations, the regional soil respiration of 416 Tg C year^{-1} is consequently much lower than the estimates of 1200 Tg C year^{-1} by Wang *et al.* (2002). This large discrepancy for regional soil respiration will apparently result in a large uncertainty in the regional net carbon budget. This suggests that the research priority should be directed to investigating the major controls on and processes of soil decomposition and carbon pool sizes as well as soil thermal and hydrological regimes under the changing climate conditions.

Impacts of soil thermal and moisture regimes on carbon dynamics on the Tibetan Plateau

On the plateau, the air temperature increased by 0.01 °C year^{-1} during the 20th century (R^2 = 0.25, P < 0.01, n = 103). The annual air temperature reached −1.3 °C in the 1990s from −2.1 °C in the 1900s while annual precipitation remained at almost the same level during the century (Fig. 2a,b). Consequently, the annual soil temperature at 20 cm depth increased by 0.01 °C year^{-1} and soil moisture deceased by 1% per year. The increasing soil temperature resulted in an increase in regional NPP of 0.52 Tg C year^{-1} and was responsible for an increase in R_H of 0.22 Tg C year^{-1}. These changes in NPP and R_H result in a regional sink of 0.3 Tg C year^{-1}. These regional carbon dynamics are correlated with the changes in climate and soil temperature and moisture during the 20th century (Table 5). Our analysis further reveals that the carbon dynamics are significantly correlated with the net nitrogen mineralization rate in the region. In particular, the correlations between NPP and NEP and NETNMIN are 0.94 and 0.93, respectively (Table 5). The warming air temperature increases soil temperature and thereby increases the soil decomposition rate and net nitrogen mineralization rate. Consequently, the increase in NETNMIN stimulates carbon uptake, promoting accumulation of vegetation and soil carbon in the region. Although the active layer depth has not significantly increased, its fluctuation due to changing climate is significantly correlated with carbon fluxes in the region (Table 5). Due to differential rates of regional NPP and R_H with increasing air temperature, the region tends to become a stronger carbon sink under warming conditions.

When soil thermal effects are not considered, NPP and R_H are modelled as functions of air temperature instead of the simulated soil temperature. Since air temperature is lower than soil temperature in spring and autumn, the simulated net nitrogen mineralization and uptake are lower, leading to a lower gross primary production and NPP. The warmer summer air

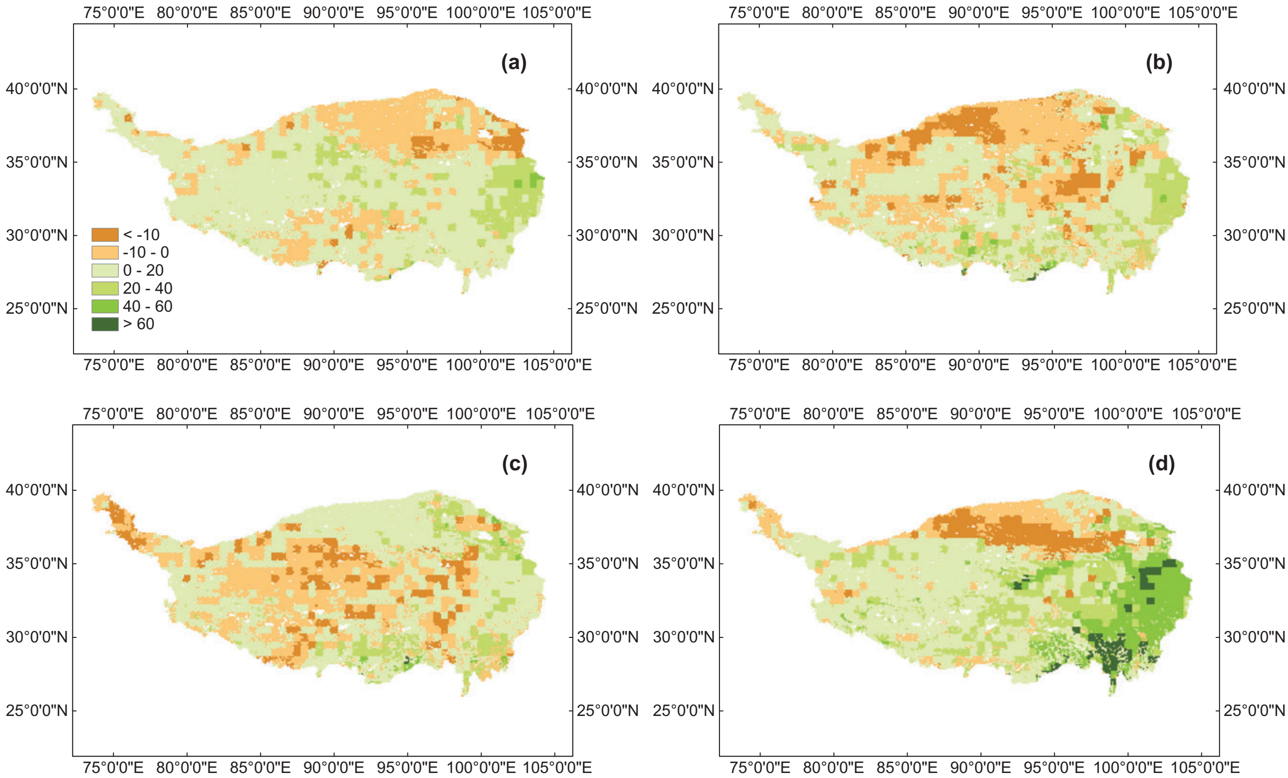

Figure 6 Spatial patterns of annual net ecosystem production (NEP) with units of g C m^{-2} year^{-1} during the 1930s (a), 1950s (b), 1970s (c) and 1990s (d). The values are simulated with the Terrestrial Ecosystem Model (TEM) considering the effects of permafrost dynamics.

Table 5 Pearson correlations between carbon pools and fluxes and physical variables on the Tibetan Plateau during the period 1901–2002. The soil temperatures are at the top 20 cm of soils.

	Air temperature	Precipitation	Soil temperature	Soil moisture	Maximum active layer depth	Net N mineralization On	Net N mineralization Off
NPP	0.38**	0.63**	0.37**	0.47**	0.19*	0.94**	0.97**
R_H	0.37**	0.63**	0.37**	0.47**	0.38**	0.93**	0.97**
NEP	0.44**	0.48**	0.42**	0.39**	0.15*	0.88**	0.84**
C_v	0.37**	0.46**	0.39**	0.13*	0.05	0.65**	0.72**
C_s	0.18*	0.38**	0.17*	0.46**	–0.05	0.85**	0.86**

*$P < 0.05$, **$P < 0.01$.

C_v and C_s are vegetation and soil carbon pools, respectively. NEP, NPP and R_H are net ecosystem production, net primary production and heterotrophic respiration, respectively. 'On' indicates that the Terrestrial Ecosystem Model (TEM) simulation has considered the effects of permafrost dynamics while 'Off' indicates that the effects have not been considered.

temperature stimulates soil respiration and nitrogen mineralization, providing more available nitrogen and leading to a higher NPP. However, the differences of the effects of air temperature and soil temperature on NPP are small in summer. As a result, the lower annual NPP and higher R_H leads to a smaller carbon sink (Table 4).

Influences of altitude, temperature and moisture gradients on carbon dynamics

On the plateau, air temperature and precipitation increase from north to south and from west to east, influenced by the Asian monsoon climate and local topography. To examine how the climate gradients affect soil temperature and moisture regimes and in turn affect carbon dynamics, we selected an east–west transect along the latitude of 30 °N and a south–north transect along the longitude of 92 °E. On the east–west transect, the elevation drops from 5000 to 3000 m in the east, annual air temperature increases from –3 °C in the west to 8 °C in the east, while annual precipitation also increases from 600 to 800 mm. These changes resulted in an increase in soil temperature of about 6 °C, but soil moisture decreases to some extent due to higher evapotranspiration from west to east. Consequently, NPP, R_H and NEP increased along the climate and altitude

Table 6 Pearson correlations between carbon fluxes and physical and chemical variables in the east–west transect (along the latitude 30 °N) and the south–north transect (along the longitude 92 °E) on the Tibetan Plateau.

		Longitude/ latitude	Elevation	Air temperature	Precipitation	Soil temperature	Soil moisture	Maximum active layer depth	Net N mineralization On	Net N mineralization Off
East–west transect	NPP	0.51**	−0.57**	0.62**	−0.03	0.60**	−0.40**	0.49**	0.97**	0.92**
(233 grid cells)	RH	0.45**	−0.54**	0.59**	−0.07	0.56**	−0.42**	0.48**	0.97**	0.94**
	NEP	0.65**	−0.59**	0.65**	0.20*	0.64**	−0.20*	0.44**	0.76**	0.64**
South–north transect	NPP	−0.75**	0.44**	0.16*	0.64**	0.15*	0.65**	−0.08	0.97**	−0.48**
(169 grid cells)	RH	−0.74**	0.41**	0.20*	0.65**	0.20*	0.60**	−0.04	0.96**	−0.49**
	NEP	−0.50**	0.52**	−0.31**	0.29**	−0.31**	0.77**	−0.39**	0.67**	−0.18*

*$P < 0.05$, **$P < 0.01$.

The values for variables are annual averages for the 1990s except for latitude, longitude and elevation. NEP, NPP and R_H are net ecosystem production, net primary production and heterotrophic respiration, respectively. 'On' indicates that the Terrestrial Ecosystem Model (TEM) simulation has considered the effects of permafrost dynamics while 'Off' indicates that the effects have not been considered.

gradient in this transect. Our statistical analysis indicates that the climate and altitude gradients are significantly correlated with the carbon dynamics in this transect (Table 6). The air temperature gradient exerts more influence than precipitation, while soil temperature and moisture have similar influences on carbon dynamics. NETNMIN increases from west to east, primarily due to the increase in soil temperature in this transect, which in turn stimulates uptake of carbon by vegetation. In addition, changes in the active layer depth of this transect remain a key factor here (Table 6).

On the south–north transect, the elevation increases from 3000 to 5000 m and then drops to 3000 m from south to north, annual air temperature decreases from 15 to −5 °C and then increases to 5 °C, while precipitation shows a sharp gradient with extremely low precipitation in the north. The annual soil temperature at 20 cm depth follows the air temperature trend and decreases from 10 to −5 °C and then increases to above 0 °C. Soil moisture dramatically drops by 20% in the north. Carbon dynamics are intimately coupled with the trends of these climatic and soil variables (Table 6). On this transect, carbon dynamics are correlated well with latitude ($R^2 > 0.48$, $P < 0.01$, $n = 169$). Similar to the east–west transect, the altitude is also a major factor on the south–north transect, suggesting the importance of considering elevation information in carbon cycling studies in the region (Table 6). Soil thermal and moisture regimes significantly affect the soil decomposition and NETNMIN, inducing carbon release from soils and stimulating carbon uptake by vegetation. Our simulations generally agree with other studies, indicating that NPP decreases from south-east to north-west due to the decreasing trend of air temperature and moisture (e.g. Piao & Fang, 2002). In contrast to the east–west transect, the active layer depth is not highly correlated with NPP and R_H dynamics in the south–north transect, but is significantly correlated with NEP dynamics (Table 6). Overall, our analysis is consistent with other findings, stating that the air temperature and precipitation are controlling factors for carbon storage on the Tibetan Plateau (Luo *et al.*, 2002). However, our study takes a further step to reveal that the changes in soil thermal and moisture conditions induced by climate change affect soil decomposition and the nitrogen mineralization processes, thereby controlling carbon dynamics in the region.

CONCLUSION

We used a process-based biogeochemistry model, TEM, to examine the changes of permafrost status and carbon cycling on the Tibetan Plateau. We first parameterized the TEM with the field data and then verified our parameterization and model using the observed data. The model and parameters were then extrapolated to the region. We find that the model is able to reproduce the distribution of permafrost on the plateau. Our simulations indicate that the region acted as a carbon sink of 36 Tg C year^{-1} in the 1990s. During the 20th century, the regional carbon dynamics showed a large inter-annual and spatial variability due to changes in climate and soil thermal and moisture regimes. Our analyses suggest that the warming temperature in this region promoted the strength of the carbon sink and shifted seasonal carbon dynamics during the century. Along the east–west transect, the NPP, soil respiration and net ecosystem productivity generally increased, primarily due to the increase in air temperature and precipitation and decrease in elevation. In contrast, the decreased carbon fluxes from south to north were primarily controlled by the precipitation gradient on the south–north transect. Our study implies that future warming will increase thawing of the permafrost, increase soil temperature and dry up soil moisture. These physical dynamics may enhance future strength of the regional carbon sink, since the rate of increase of NPP is higher than that of soil respiration on the Tibetan Plateau. Further, our study indicates that the future quantification of regional carbon dynamics in this climate-sensitive region should take the effects of soil thermal dynamics into account.

ACKNOWLEDGEMENTS

This study is supported by Q. C. Wong's research fund. The research is also supported in part by the National Science Foundation (NSF-0554811) and the National Nature Science Foundation of China (project no. 40701008). The high-performance computing for this research was provided by the Rosen Center for Advanced Computing at Purdue University.

REFERENCES

Balshi, M.S., McGuire, A.D., Zhuang, Q., Melillo, J.M., Kicklighter, D.W., Kasischke, E., Wirth, C., Flannigan, M., Harden, J., Clein, J.C., Burnside, T.J., McAllister, J., Kurz, W.A., Apps, M. & Shvidenko, A. (2007) The role of historical fire disturbance in the carbon dynamics of the pan-boreal region: a process-based analysis. *Journal of Geophysical Research*, **112**, G02029.

Belward, A.S., Estes, J.E. & Kline, K.D. (1999) The IGBP-DIS global 1-km land-cover data set DISCover: a project overview. *Photogrammetric Engineering and Remote Sensing*, **65**, 1013–1020.

Brown, J., Ferrians, Jr, O.J., Heginbottom, J.A. & Melnikov, E.S. (1998) *Circum-Arctic map of permafrost and ground-ice conditions*, revised February 2001. National Snow and Ice Data Center/World Data Center for Glaciology, Digital Media, Boulder, CO.

Du, J. (2001) Change of temperature in Tibetan Plateau from 1961 to 2000. *Acta Geographica Sinica*, **56**, 6, 682–690 (in Chinese).

Euskirchen, E.S., McGuire, A.D., Kicklighter, D.W., Zhuang, Q., Clein, J.S., Dargaville, R.J., Dye, D.G., Kimball, J.S., McDonald, K.C., Melillo, J.M., Romanovsky, V.E. & Smith, N.V. (2006) Importance of recent shifts in soil thermal dynamics on growing season length, productivity, and carbon sequestration in terrestrial high-latitude ecosystem. *Global Change Biology*, **12**, 731–750.

Fang, J., Liu, G. & Xu, S. (1996) C pool of terrestrial ecosystem in China. *Monitoring of greenhouse gas concentration and emission and relevant processes* (ed. by G. Wang and Y. Wen), pp. 109–128. China Environmental Science Press, Beijing (in Chinese).

Farr, T.G., Rosen, P.A., Caro, E., Crippen, R., Duren, R., Hensley, S., Kobrick, M., Paller, M., Rodriguez, E., Roth, L., Seal, D., Shaffer, S., Shimada, J., Umland, J., Werner, M., Oskin, M., Burbank, D. & Alsdorf, D. (2007) The Shuttle Radar Topography Mission. *Reviews of Geophysics*, **45**, RG2004, doi:10.1029/2005RG000183.

Feng, S., Tang, M. & Wang, D. (1998) New evidence for the Qinghai-Xizang (Tibet) Plateau as a pilot region of climatic fluctuation in China. *Chinese Science Bulletin*, **43**, 20, 1745–1749.

Food and Agriculture Organization-United Nations Educational, Scientific, and Cultural Organization (FAO-UNESCO) (1971) *Soil map of the world, 1:5,000,000*. FAO, Paris.

Kato, T., Tang, Y., Gu, S., Cui, X., Hirota, M., Du, M., Li, Y., Zhao, X. & Oikawa, T. (2004a) Carbon dioxide exchange between the atmosphere and an alpine meadow ecosystem on the Qinghai-Tibetan Plateau. *China Agricultural and Forest Meteorology*, **124**, 121–134.

Kato, T., Tang, Y., Gu, S., Hirota, M., Cui, X., Du, M., Li, Y., Zhao, X. & Oikawa, T. (2004b) Seasonal patterns of gross primary production and ecosystem respiration in an alpine meadow ecosystem on the Qinghai-Tibetan Plateau. *Journal of Geophysical Research*, **109**, D12109.

Kato, T., Tang, Y., Gu, S., Hirota, M., Du, M., Li, Y. & Zhao, X. (2006) Temperature and biomass influences on interannual changes in CO_2 exchange in an alpine meadow on the Qinghai-Tibetan Plateau. *Global Change Biology*, **12**, 1285–1298.

Li, S. (1993) Agroclimatic resources and agricultural distribution patterns. *Climate and agriculture in China* (ed. by C. Cheng), pp. 30–69. China Meteorological Press, Beijing (in Chinese).

Li, Z., Yu, G., Xiao, X., Li, Y., Zhao, X., Ren, C., Zhang, L. & Fu, Y. (2007) Modeling gross primary production of alpine ecosystems in the Tibetan Plateau using MODIS images and climate data. *Remote Sensing of Environment*, **107**, 510–519.

Loveland, T.R., Reed, B.C., Brown, J.F., Ohlen, D.O., Zhu, Z., Yang, L. & Merchant, J.W. (2000) Development of a global land cover characteristics database and IGBP DISCover from 1 km AVHRR data. *International Journal of Remote Sensing*, **21**, 1303–1330.

Lu, J. & Ji, J. (2002) A simulation study of atmosphere–vegetation interaction over the Tibetan Plateau: net primary productivity and leaf area index. *Chinese Journal of Atmospheric Sciences*, **26**, 255–262 (in Chinese).

Luo, T., Li, W., Leng, Y.F. & Yue, Y. (1998) Estimation of total biomass and potential distribution of net primary productivity in the Tibetan Plateau. *Geographical Research*, **17**, 337–344 (in Chinese).

Luo, T., Shi, S., Luo, J. & Ouyang, H. (2002) Distribution patterns of aboveground biomass in Tibetan alpine vegetation transects. *Acta Phytoecologica Sinica*, **26**, 668–676 (in Chinese).

Luo, T., Pan, Y., Ouyang, H., Shi, P., Luo, J., Yu, Z. & Lu, Q. (2004) Leaf area index and net primary productivity along subtropical to alpine gradients in the Tibetan Plateau. *Global Ecology and Biogeography*, **13**, 345–358.

Luo, T., Brown, S., Pan, Y., Shi, P., Ouyang, H., Yu, Z. & Zhu, H. (2005a) Root biomass along subtropical to alpine gradients: global implication from Tibetan transect studies. *Forest Ecology and Management*, **206**, 349–363.

Luo, T., Luo, J. & Pan, Y. (2005b) Leaf traits and associated ecosystem characteristics across subtropical and timberline forests in the Gongga Mountains, eastern Tibetan Plateau. *Oecologia*, **142**, 261–273.

McGuire, A.D., Melillo, J.M., Joyce, L.A., Kicklighter, S.W., Grace, A.L., Moore, B., III & Vörösmarty, C.J. (1992) Interactions between carbon and nitrogen dynamics in estimating net primary productivity for potential vegetation in North America. *Global Biogeochemical Cycles*, **6**, 101–124.

McGuire, A.D., Melillo, J.M., Kicklighter, D.W., Pan, Y., Xiao, X., Helfrich, J., Moore, B., III, Vörösmarty, C.J. & Schloss, A.L. (1997) Equilibrium responses of global net primary production and carbon storage to doubled atmospheric carbon

dioxide: sensitivity to changes in vegetation nitrogen concentration. *Global Biogeochemical Cycles*, **11**, 173–189.
Melillo, J.M., McGuire, A.D., Kicklighter, D.W., Moore, B., III, Vörösmarty, C.J. & Schloss, A.L. (1993) Global climate change and terrestrial net primary production. *Nature*, **363**, 234–240.
Mitchell, T.D. & Jones, P.D. (2005) An improved method of constructing a database of monthly climate observations and associated high-resolution grids. *International Journal of Climatology*, **25**, 693–712.
Ni, J. (2000) A simulation of biomes on the Tibetan Plateau and their responses to global climate change. *Mountain Research and Development*, **20**, 80–89.
Oelke, C. & Zhang, T. (2007) Modeling the active-layer depth over the Tibetan Plateau. *Arctic, Antarctic, and Alpine Research*, **39**, 714–722.
Paetzold, R., Lin, Z. & Ping, C. (2003) Monthly summaries of soil temperature and soil moisture at sites in China. National Snow and Ice Data Center/World Data Center for Glaciology. Available at: http://nsidc.org/data/ggd625.html (accessed 20 September 2009).
Pan, Y., Melillo, J.M., McGuire, A.D., Kicklighter, D.W., Pitelka, L.F., Hibbard, K., Pierce, L.L., Running, S.W., Ojima, D.S., Parton, W.J., Schimel, D.S. & other VEMAP members (1998) Modeled responses of terrestrial ecosystems to elevated atmospheric CO_2: a comparison of simulation be the biogeochemistry models of the Vegetation/Ecosystem Modeling and Analysis Project (VEMAP). *Oecologia*, **114**, 389–404.
Piao, S. & Fang, J. (2002) Terrestrial net primary production and its spatio-temporal patterns in Qinghai-Xizang Plateau, China during 1982–1999. *Journal of Natural Resources*, **17**, 373–380 (in Chinese).
Piao, S., Fang, J. & He, J. (2006) variations in vegetation net primary production in the Qinghai-Xizang plateau, China, from 1982 to 1999. *Climatic Change*, **74**, 253–267.
Qiu, G., Zhou, Y., Guo, D. & Wang, Y. (2002) *Maps of geocryological regions and classifications*, digitized by T. Zhang. National Snow and Ice Data Center/World Data Center for Glaciology, Boulder, CO.
Raich, J.W., Rastetter, E.B., Mellilo, J.M., Kicklighter, D.W., Steudler, P.A., Peterson, B.J., Grace, A.L., Moore, B., III & Vörösmarty, C.J. (1991) Potential net primary productivity in South America: application of a global model. *Ecological Applications*, **1**, 399–429.
Wang, G., Cheng, G. & Shen, Y. (2002) Soil organic pool of grasslands on the Tibetan Plateau and its global implication. *Journal of Glaciology and Geography*, **21**, 695–700 (in Chinese).
Wang, J., Hu, D. & Sun, Z. (2003) Simulation of terrestrial C cycle balance model in Tibet. *Journal of Geographical Sciences*, **13**, 316–322.
Wang, S., Jin, H., Li, S. & Zhao, L. (2000) Permafrost degradation on the Qinghai-Tibet Plateau and its environmental impacts. *Permafrost and Periglacial Processes*, **11**, 43–53.
Zhang, Y., Li, B. & Zheng, D. (2002) A discussion on the boundary and area of the Tibetan Plateau in China. *Geographical Research*, **21**, 1–8 (in Chinese).
Zheng, D. (1996) The system of physico-geographical regions of the Qinghai-Xizang (Tibeta) Plateau. *Science in China (Series D)*, **39**, 410–417.
Zhou, C., Ouyang, H., Wang, Q. & Watanabe, M. (2004) Estimation of net primary productivity in Tibetan Plateau. *Acta Geographica Sinica*, **59**, 74–79 (in Chinese).
Zhuang, Q., Romanovsky, V.E. & McGuire, A.D. (2001) Incorporation of a permafrost model into a large-scale ecosystem model: evaluation of temporal and spatial scaling issues in simulating soil thermal dynamics. *Journal of Geophysical Research*, **106**, 33648–33670.
Zhuang, Q., McGuire, A.D., O'Neill, K.P., Harden, J.W., Romanovsky, V.E. & Yarie, J. (2002) Modeling the soil thermal and carbon dynamics of a fire chronosequence in Interior Alaska. *Journal of Geophysical Research*, **107**, 8147, doi:10.1029/2001JD001244. [print 108(D1), 2003].
Zhuang, Q., McGuire, A.D., Melillo, J.M., Clein, J.S., Dargaville, R.J., Kicklighter, D.W., Myneni, R.B., Dong, J., Romanovsky, V.E., Harden, J. & Hobbie, J.E. (2003) Carbon cycling in extratropical terrestrial ecosystems of the Northern Hemisphere during the 20th century: a modeling analysis of the influences of soil thermal dynamics. *Tellus*, **55B**, 751–776.
Zhuang, Q., Melillo, J.M., Sarofim, M.C., Kicklighter, D.W., McGuire, A.D., Felzer, B.S., Sokolov, A., Prinn, R.G., Steudler, P.A. & Hu, S. (2006) CO_2 and CH_4 exchanges between land ecosystems and the atmosphere in northern high latitudes over the 21st century. *Geophysical Research Letters*, **33**, L17403, doi:10.1029/2006GL026972.

SUPPORTING INFORMATION

Additional Supporting Information may be found in the online version of this article:

Appendix S1 Values and sources for estimated pools and fluxes used to parameterize the ecosystem models.

As a service to our authors and readers, this journal provides supporting information supplied by the authors. Such materials are peer-reviewed and may be re-organized for online delivery, but are not copy-edited or typeset. Technical support issues arising from supporting information (other than missing files) should be addressed to the authors.

BIOSKETCHES

Qianlai Zhuang (PhD, University of Alaska Fairbanks) is an associate professor in the Department of Earth and Atmospheric Sciences and Department of Agronomy at Purdue University, West Lafayette, IN. His research interests focus on studying biogeochemical dynamics with process-based biogeochemistry models.

Editor: Wolfgang Cramer